

Application of Minimal Subtraction Renormalization to Crossover Behavior near the ^3He Liquid-Vapor Critical Point

Fang Zhong, M. Barmatz, and Inseob Hahn

Jet Propulsion Laboratory, California Institute of Technology, Pasadena, California 91109-8099

(Dated: October 24, 2018)

Parametric expressions are used to calculate the isothermal susceptibility, specific heat, order parameter, and correlation length along the critical isochore and coexistence curve from the asymptotic region to crossover region. These expressions are based on the minimal-subtraction renormalization scheme within the ϕ^4 model. Using two adjustable parameters in these expressions, we fit the theory globally to recently obtained experimental measurements of isothermal susceptibility and specific heat along the critical isochore and coexistence curve, and early measurements of coexistence curve and light scattering intensity along the critical isochore of ^3He near its liquid-vapor critical point. The theory provides good agreement with these experimental measurements within the reduced temperature range $|t| \leq 2 \times 10^{-2}$.

I. INTRODUCTION

It is well known that thermodynamic quantities exhibit singularities asymptotically close to the critical point. The power-law behavior of these singularities, characterized by critical exponents and the concept of universality and scaling, have been successfully described by renormalization-group (RG) theory. Away from the asymptotic region, thermodynamic quantities of real physical systems deviate from simple power-law behavior. However, RG theory can still provide insight in understanding critical crossover behavior.

There are two main field-theoretical renormalization-group schemes to treat critical-to-classical crossover phenomena. Dohm and co-workers developed the minimal-subtraction renormalization (MSR) scheme [1] while Bagnuls and Bervillier developed the massive renormalization (MR) scheme [2]. Both of these theories used the Borel resummation technique to describe the crossover behavior of the ϕ^4 model in any $O(n)$ universality class and in three dimensions. The difference between the two schemes was discussed in ref.[1]. These field-theoretical crossover theories were improved over the years as asymptotic theories became more accurate [3]. Recently, Larin *et al.* improved the MSR expressions for the specific heat and compared their results with the superfluid helium ($n = 2$) system [4]. Bagnuls and Bervillier have also improved their theory to match the recent asymptotic values for exponents and leading amplitude ratios [5]. Both renormalization schemes can provide crossover functional forms for thermal properties with a minimal set of fluid-dependent adjustable parameters. However, a direct comparison between these recent theoretical predictions and different experimental measurements near the liquid-vapor critical point ($n = 1$) has been lacking.

In this paper we will present a direct comparison between the MSR field theoretical crossover functions and various experimental measurements near the liquid-gas critical point of ^3He . The comparison using the MR theory will be published elsewhere.

The paper is divided into two parts. In the first part, we briefly summarize the MSR functional expressions for susceptibility, specific heat, coexistence curve, and correlation length from previous work [1, 6, 7, 8]. In addition, we derived within the MSR framework new RG functional expressions for the asymptotic critical amplitudes of the susceptibility and coexistence curve as well as the first coefficient in a Wegner expansion for susceptibility, specific heat, coexistence curve, and correlation length. From these expressions, universal amplitude ratios for the $O(1)$, 3-dimensional system are calculated and compared with the most recent values from Bagnuls *et al.* [5] and Fisher *et al.* [9].

The second part of the paper includes the results of MSR functional fits to experimental measurements. In our previous work, we analyzed the isothermal susceptibility of ^3He along the critical isochore above T_c using theoretical expressions based upon the minimal-subtraction scheme [10]. In this work, we combine that analysis with susceptibility measurements along the coexistence curve and specific heat measurements along the critical isochore [11]. Measurements of coexistence curve and the light scattering intensity near the critical point of ^3He [12, 13] are also analyzed.

II. THEORETICAL EXPRESSIONS

The Hamiltonian for the ϕ^4 model in three dimensions ($d = 3$) is

$$H_\phi = \int d^3x \left\{ \frac{1}{2} r_0 \phi_0^2 + \frac{1}{2} (\nabla \phi_0)^2 + u_0 \phi_0^4 \right\}, \quad (1)$$

where ϕ_0 is the order parameter field, whose statistical mean value is the physical order parameter of a given system. The parameter u_0 is the fourth-order coupling constant. The parameter r_0 is related to the reduced temperature $t \equiv (T - T_c)/T_c$ by

$$r_0 = a_0 t, \quad (2)$$

where a_0 is a nonuniversal constant. It is important to note that the total Hamiltonian is the sum of $H = H_\phi + H_0$, where H_0 is the analytic background free energy. Since the liquid-vapor critical point has a single component order parameter and belongs to the $O(1)$ universality class, we have $n = 1$.

The dimensionless bare order parameter field ϕ_0 and the bare coupling parameters u_0 and r_0 are renormalized to [Eqs. (S2.11) and (S2.12) [6]]

$$\phi = Z_\phi(u, \epsilon)^{-1/2} \phi_0 \quad (3)$$

$$u = \mu^{-1} Z_u(u, \epsilon)^{-1} Z_\phi(u, \epsilon)^2 A_3 u_0 \quad (4)$$

$$r = a t = Z_r(u, \epsilon)^{-1} a_0 t, \quad (5)$$

where $A_3 = (4\pi)^{-1}$ is a geometric factor and $\epsilon = 4 - d = 1$ for dimension $d = 3$. The Z factors are associated with their respective field-theoretic functions [1]

$$\zeta_r(u) = \mu \partial_\mu \ln Z_r(u, \epsilon)^{-1} \Big|_0, \quad (6)$$

$$\zeta_\phi(u) = \mu \partial_\mu \ln Z_\phi(u, \epsilon)^{-1} \Big|_0, \quad (7)$$

$$\beta_u(u) = u \left[-1 + \mu \partial_\mu (Z_u^{-1} Z_\phi^2) \Big|_0 \right], \quad (8)$$

where the index 0 means differentiation at fixed r_0 , ϕ_0 , and u_0 .

By introducing a flow parameter l , the effective coupling $u(l)$ satisfies the flow equation

$$l \frac{du(l)}{dl} = \beta_u(u(l)). \quad (9)$$

The flow parameter l is related to the correlation length by

$$\xi(l) = (\mu l)^{-1}, \quad (10)$$

with μ^{-1} being an arbitrary reference length. The flow parameter $l = 0$ corresponds to the Ising fixed point $u(l = 0) = u^*$, which is determined from $\beta_u(u^*) = 0$. The effective coupling $r(l)$ satisfies the flow equation

$$l \frac{dr(l)}{dl} = r(l) \zeta_r(u(l)). \quad (11)$$

The flow parameter $l = 1$ is an arbitrary reference point, at which the nonuniversal initial values are $u(l = 1) = u$ and $r(l = 1) = r = a t$.

The field-theoretic functions $\zeta_r(u)$, $\zeta_\phi(u)$ and $\beta_u(u)$ in Eqs. (6)-(8) are known up to five-loop order in perturbation expansions around $u = 0$ [1]. However, the expansions do not converge away from $u = 0$. Hence Borel resummations were used on the expansions to calculate the values of these functions over the range $0 < u \leq u^*$. For most investigations, see for instance ref.[6, 7, 8], only the function values at the fixed point u^* were calculated using the Borel resummations on the five-loop expansions. The function values over the range $0 < u < u^*$ were obtained using up to two-loop order expressions with extrapolation terms added in order to reproduce the values at the fixed point [1]. For a system of dimension $d = 3$ and single component order-parameter $n = 1$, one obtains

$$\zeta_r(u) = 12u - 120u^2 + a_1 u^3 - a_2 u^4, \quad (12)$$

$$\zeta_\phi(u) = -24u^2 + a_3 u^3, \quad (13)$$

$$\beta_u(u) = -u + 36u^2(1 + a_4 u)/(1 + a_5 u). \quad (14)$$

Here a_1 through a_5 are the coefficients for the extrapolation terms with values listed in Appendix A. Using these functions and the flow equations, thermal properties along the critical isochore and coexistence curve can be calculated from the asymptotic to crossover regions using the initial values for Eqs. (9) and (11), $u = u(l = 1)$ and $a = a(l = 1)$, and the arbitrary length scale μ^{-1} in Eq. (10).

A. Reduced temperature

Within the MSR scheme, the expression for the reduced temperature in terms of the flow parameter l can be derived as follows. The reduced temperature t and the flow parameter l can be linked using Eqs. (S4.25), and (S4.26) in ref.[1] and Eq. (H2.9) of ref.[7], together with the solution of Eq. (11)

$$\begin{aligned} r(l) &= r(1) \exp \int_1^l \zeta_r \frac{dl'}{l'} \\ &= a |t| \exp \int_1^l \zeta_r \frac{dl'}{l'} \\ &= b_\pm(u(l)) \mu^2 l^2, \end{aligned} \quad (15)$$

with

$$b_+(u(l)) = Q(u(l)), \quad (16)$$

$$b_-(u(l)) = \frac{3}{2} - Q(u(l)). \quad (17)$$

Here ‘+’ is for $T > T_c$ and ‘-’ is for $T < T_c$. Krause *et al.* [8] determined a one-loop expression

plus a higher-order extrapolation for $Q(u)$ given by [Eq. (K3.5)]

$$Q(u) = 1 + b_Q u^2 \ln(c_Q u), \quad (18)$$

where b_Q and c_Q are the extrapolation coefficients with the values given in Table III in Appendix A.

By adding and subtracting $\zeta_r^* = \zeta_r(u^*)$ in the integrand of Eq. (15) and using the identity $\nu^{-1} = 2 - \zeta_r^*$, where ν is the critical exponent of correlation length ξ , one arrives at

$$a |t| \exp \int_1^l (\zeta_r - \zeta_r^*) \frac{dl'}{l'} = b_{\pm}(l) \mu^2 l^{1/\nu}. \quad (19)$$

By rearrange Eq. (19), one obtains the following expression for the reduced temperature

$$|t| = b_{\pm}(l) t_0 l^{1/\nu} \exp[-F_r(l)], \quad (20)$$

with

$$t_0 = \frac{\mu^2}{a} \exp[F_r(1)], \quad (21)$$

and

$$\begin{aligned} F_r(l) &= \int_0^l \frac{dl'}{l'} [\zeta_r(u(l')) - \zeta_r(u^*)] \\ &= \int_{u^*}^{u(l)} \frac{\zeta_r(u') - \zeta_r(u^*)}{\beta_u(u')} du'. \end{aligned} \quad (22)$$

B. Susceptibility

1. General expression

The following expressions for the dimensionless susceptibility $\chi_T^* \equiv \chi_{\pm}$ were given in refs. [7, 8] respectively for $T > T_c$ [Eq. (K2.7)] and $T < T_c$ [Eq. (H2.16)],

$$\chi_{\pm} = \frac{Z_{\phi}(u)}{\mu^2 l^2 f_{\pm}(u(l))} \exp \int_l^1 \zeta_{\phi} \frac{dl'}{l'}. \quad (23)$$

The amplitude functions, f_{\pm} , were expressed to two-loop order plus a higher-order extrapolation, [Eqs. (K3.1) and (H4.2)], to give

$$f_+[u] = 1 - \frac{92}{9} u^2 (1 + b_{\chi} u) \quad (T > T_c), \quad (24)$$

$$f_-[u] = [1 - 18u + 159.56u^2 (1 + d_{\chi} u)]^{-1} \quad (T < T_c),$$

where b_{χ} and d_{χ} are the extrapolation coefficients with the values given in Table III in Appendix A.

The minimal renormalization factor, Z_{ϕ} , in Eq. (23) is given by [Eq. (K A12)]

$$Z_{\phi}(u)^{-1} = \exp \int_0^u du' \frac{\zeta_{\phi}(u')}{\beta_u(u')}. \quad (25)$$

The expression

$$\chi_{\pm} = \chi_0 l^{-\gamma/\nu} \frac{\exp[-F_{\phi}(u(l))]}{f_{\pm}(u(l))} \quad (26)$$

can be obtained by adding and subtracting $\zeta_{\phi}^* = \zeta_{\phi}(u^*)$ in the integrand of Eq. (23), and using the relations $\zeta_{\phi}^* = -\eta$ [1] and $\gamma = \nu(2 - \eta)$, where η is the critical exponent of the fluctuation correlation at the critical point and γ is the critical exponent of susceptibility. In Eq. (26)

$$\chi_0 = \mu^{-2} Z_{\phi}(u) \exp[F_{\phi}(1)], \quad (27)$$

and

$$\begin{aligned} F_{\phi}(l) &= \int_0^l \frac{dl'}{l'} [\zeta_{\phi}(u(l')) - \zeta_{\phi}(u^*)] \\ &= \int_{u^*}^{u(l)} \frac{\zeta_{\phi}(u') - \zeta_{\phi}(u^*)}{\beta_u(u')} du'. \end{aligned} \quad (28)$$

Using Eq. (10) and $\gamma = \nu(2 - \eta)$, Eq. (26) can be rewritten as

$$\chi_{\pm} = \xi^{2-\eta} \chi_0 \mu^{2-\eta} \frac{\exp[-F_{\phi}(u(l))]}{f_{\pm}(u(l))}. \quad (29)$$

Thus, in the asymptotic regime ($F_{\phi} \rightarrow 0$)

$$\chi_{\pm} = D \xi^{2-\eta} \quad (30)$$

with a nonuniversal proportionality constant $D \equiv \chi_0 \mu^{2-\eta} f_{\pm}^{-1}(u^*)$.

2. Critical Amplitudes

Within the pure ϕ^4 model, the standard Wegner expansion for the susceptibility is given by

$$\chi_{\pm} = \Gamma_0^{\pm} |t|^{-\gamma} (1 + \Gamma_1^{\pm} |t|^{\Delta} + \Gamma_2^{\pm} |t|^{2\Delta} + \dots), \quad (31)$$

where Γ_0^{\pm} are the leading asymptotic critical amplitudes, Γ_1^{\pm} are the first Wegner expansion amplitudes above and below the transition, and Δ is the correction-to-scaling exponent. The details of the derivations of the leading and first Wegner critical amplitudes are given in Appendix B. Here we list the derived expressions for the critical amplitudes,

$$\Gamma_0^{\pm} = \frac{\chi_0 (b_{\pm}^* t_0)^{\gamma}}{f_{\pm}(u^*)}, \quad (32)$$

$$\Gamma_1^{\pm} = \left(\gamma \frac{\zeta_r'}{\omega} - \gamma \frac{b'_{\pm}}{b_{\pm}} + \frac{\zeta_{\phi}'}{\omega} + \frac{f'_{\pm}}{f_{\pm}} \right) \Big|_{u^*} \frac{u^* - u}{(b_{\pm}^* t_0)^{\Delta}} \quad (33)$$

with $\Delta = \nu\omega$ and $\omega = d\beta_u/du|_{u^*}$.

C. Specific Heat

1. General expressions

The total specific heat is usually separated as

$$C^\pm = C_B + C_\phi^\pm, \quad (34)$$

where the term $C_B > 0$ represents an analytic ‘‘background’’ contribution from the analytic background free energy H_0 , and C_ϕ^\pm represents the critical contribution from order parameter fluctuations. Here ‘+’ is for the specific heat above T_c along the critical isochore, ‘-’ is for below T_c in coexisting phases.

The critical specific heat C_ϕ^\pm derived from the Hamiltonian expressed in Eq. (1) has two representations within the MSR scheme. These two representations are derived via multiplicative and additive renormalization as detailed in ref. [6]. The most recent work by Larin *et al.*[4] used the representation via additive renormalization that we will use in this paper.

The critical specific heat C_ϕ^\pm per unit volume near T_c is expressed by [Eqs. (S2.36) or (L3.3)][4, 6]

$$C_\phi^\pm = T_c^2 V^{-1} \frac{\partial^2}{\partial T^2} \ln \int D\phi \exp -H_\phi \quad (35)$$

$$= \frac{1}{4} a^2 \mu^{-1} A_3 K_\pm(u(l)) \exp \int_u^{u(l)} \frac{2\zeta_r(u') - 1}{\beta_u(u')} du'.$$

The amplitude functions $K_\pm(u)$ are given by

$$K_\pm(u) = F_\pm(u) - A(u). \quad (36)$$

The functions $F_\pm(u)$ for $n = 1$ can be expressed by a two-loop calculation plus a higher-order extrapolation, [Eqs. (K3.4) [8] and (H4.4)[7]]

$$F_\pm[u] = \begin{cases} -1 - 6u(1 + b_F u) & (T > T_c) \\ (2u)^{-1} - 4(1 + d_F u) & (T < T_c) \end{cases}, \quad (37)$$

where b_F and d_F are the extrapolation coefficients with the values given in Table III in Appendix A. The function $A(u)$ in Eq. (36) is governed by

$$l \frac{dA(u(l))}{dl} = 4B(u(l)) + \{1 - 2\zeta_r(u(l))\} A(u(l)), \quad (38)$$

with $A(u = 0) = -4B(u = 0)$. The function $B(u)$ has been calculated to $O(u^5)$ for any given n [Eq. (L2.21)] [4]. However the five-loop Borel resummation of $B(u)$ was only performed for $n = 1$ at u^* . Hence a new extrapolation term with a coefficient b_B is added to the two-loop expression [4] in order to satisfy $B(u^*, n = 1)$,

$$B(u) = \frac{1}{2} + 9(1 + b_B u)u^2. \quad (39)$$

At the fixed point $u = u^*$, $ldA(u(l))/dl = \beta_u(u)dA(u)/du = 0$ since $\beta_u(u^*) = 0$, and Eq. (38) leads to

$$A^* \equiv A(u^*) = -\frac{4\nu B(u^*)}{\alpha}, \quad (40)$$

where $2\zeta_r^* - 1 \equiv -\alpha/\nu$ [1] is used with α being the critical exponent for specific heat at constant volume.

The integral in the exponential of Eq. (35) can be rewritten as

$$\int_1^l \frac{dl'}{l'} (2\zeta_r - 1) = 2 \int_1^l \frac{dl'}{l'} (\zeta_r - \zeta_r^*) + \ln l^{-\alpha/\nu} \quad (41)$$

using $2\zeta_r^* - 1 \equiv -\alpha/\nu$. The expression for the specific heat from the additive renormalization can now be rewritten as

$$C_\phi^\pm = \frac{a^2}{16\pi\mu} K_\pm(l) l^{-\alpha/\nu} \exp[2F_r(l)] \exp[-2F_r(1)]$$

$$= C_0 l^{-\alpha/\nu} \exp[2F_r(l)] K_\pm(u(l)), \quad (42)$$

where $F_r(l)$ is given by Eq. (22) and C_0 is defined as

$$C_0 \equiv \frac{a^2}{16\pi\mu} \exp[-2F_r(1)] = \frac{\mu^3}{16\pi t_0^2}. \quad (43)$$

2. Critical Amplitudes

The standard Wegner expansion within the pure ϕ^4 model for specific heat can be written as

$$C^\pm = A_0^\pm |t|^{-\alpha} (1 + A_1^\pm |t|^\Delta + A_2^\pm |t|^{2\Delta} + \dots)$$

$$+ B_{cr} + C_B \quad (44)$$

where B_{cr} is a constant background induced by long-range correlations between the fluctuations. The experimentally measured constant background is the sum of B_{cr} and the analytic background, C_B .

The expression for the Wegner expansion of the specific heat via multiplicative renormalization was derived and given in Eqs. (S4.23) and (S4.24) of ref. [6]. In Appendix C, we derive the expressions for the critical amplitudes and the critical background, B_{cr} , for the representation via additive renormalization, using the technique that is consistent with the one used for susceptibility. The results of these derivations are,

$$A_0^\pm = C_0 (b_\pm^* t_0)^\alpha (F_\pm^* - A^*), \quad (45)$$

$$A_1^\pm = \left[\frac{1}{A^* - F_\pm^*} \left(F_\pm' - \frac{2\nu}{\Delta - \alpha} (2B' - A^* \zeta_r') \right) \right.$$

$$\left. - (2 - \alpha) \frac{\zeta_r'}{\omega} - \alpha \frac{b_\pm'}{b_\pm} \right] \Big|_{u^*} \frac{u^* - u}{(b_\pm^* t_0)^\Delta}, \quad (46)$$

$$-\frac{B_{cr}}{C_0} = A(u) - A^* + \frac{2\nu}{\Delta - \alpha}(2B' - A^*\zeta'_r)(u^* - u). \quad (47)$$

The variables with a prime in Eqs. (46) and (47) are derivatives with respect to u . The right hand side of Eq. (47) is negative for any given u . Hence one has $B_{cr} < 0$ since $C_0 > 0$ from Eq. (43).

D. Coexistence curve

1. General expressions

In the liquid-vapor coexisting phases below T_c , the density difference $\Delta\rho_{L,V} \equiv \rho_{L,V}/\rho_c - 1$ is the statistical mean of the order parameter field $\langle\phi\rangle$. There is no asymmetry between $\Delta\rho_L$ and $\Delta\rho_V$ within the ϕ^4 model. Schloms and Dohm have given an expression for the square of the physical order parameter [Eq. (S3.10)] [6],

$$\langle\phi\rangle^2 = A_3 Z_\phi(u) f_\phi(u(l_-)) \xi_-^{-1} \exp \int_{l_-}^1 \zeta_\phi \frac{dl'}{l'}. \quad (48)$$

Here $Z_\phi(u)$ is given in Eq. (25). The amplitude function $f_\phi(u)$ is expanded in one-loop with an extrapolation term, [Eq. (H4.1)] [7], to yield

$$f_\phi(u) = (8u)^{-1} (1 + d_\phi u). \quad (49)$$

The correlation length below T_c is linked to the flow parameter by $l_- = (\mu\xi_-)^{-1}$. By combining these expressions and following the derivation of Eq. (26), one has

$$\langle\phi\rangle^2 = \phi_0^2 l_-^{2\beta/\nu} f_\phi(u(l_-)) \exp[-F_\phi(l_-)], \quad (50)$$

where $1 + \eta = 2\beta/\nu$ is used and

$$\phi_0^2 = (4\pi)^{-1} \mu Z_\phi(u) \exp[F_\phi(1)], \quad (51)$$

with β being the critical exponent of the order parameter.

2. Critical Amplitudes

Using Eq. (20) to replace $l_-^{2\beta/\nu}$ in Eq. (50) and the scaling relations $\gamma = \nu(2 - \eta)$, $\alpha = 2 - 3\nu$, and $\alpha + 2\beta + \gamma = 2$, one has

$$\langle\phi\rangle = \pm \phi_0 t_0^{-\beta} |t|^\beta [b_-(l_-)]^{-\beta} [f_\phi(l_-)]^{1/2} \times \exp[\beta F_r(l_-)] \exp[-F_\phi(l_-)/2]. \quad (52)$$

Expanding $b_-(l_-)$, $f_\phi(l_-)$, $F_r(l_-)$, and $F_\phi(l_-)$ in the same manner as described in Appendix B, one obtains the Wegner expansion for coexistence curve,

$$\Delta\rho_{L,V} = \pm B_0 |t|^\beta (1 + B_1 |t|^\Delta), \quad (53)$$

with the leading critical amplitude and the first Wegner amplitude being respectively

$$B_0 = \phi_0 (b_-^* t_0)^{-\beta} (f_\phi^*)^{1/2} \quad (54)$$

$$B_1 = \left(\beta \frac{b'_-}{b_-} - \beta \frac{\zeta'_r}{\omega} - \frac{f'_\phi}{2f_\phi} + \frac{\zeta'_\phi}{2\omega} \right) \Big|_{u^*} \frac{u^* - u}{(b_-^* t_0)^\Delta}. \quad (55)$$

E. Correlation length

Using Eq. (20) to express l in terms of $|t|$, the expression for dimensionless correlation length (if μ^{-1} is taken dimensionless) is derived from Eq. (10) as

$$\xi |t|^\nu = \mu^{-1} [b_\pm(u(l))t_0]^\nu \exp[-\nu F_r(l)]. \quad (56)$$

An expansion of Eq. (56) around $u(l) \sim u^*$ to $O[(u - u^*)^2]$ leads to

$$\xi_\pm |t|^\nu = \mu^{-1} (b_\pm^* t_0)^\nu \times \left[1 + \nu \left(\frac{\zeta'_r}{\omega} - \frac{b'_\pm}{b_\pm} \right) \Big|_{u^*} \frac{u^* - u}{(b_\pm^* t_0)^\Delta} |t|^\Delta \right]. \quad (57)$$

This equation is identical to Eq. (S4.8) of ref.[6]. By comparing Eq. (57) to the standard Wegner expansion form,

$$\xi |t|^\nu = \xi_0^\pm (1 + \xi_1^\pm |t|^\Delta), \quad (58)$$

one obtains the leading amplitudes and first Wegner correction amplitudes of the correlation length

$$\xi_0^\pm = \mu^{-1} (b_\pm^* t_0)^\nu, \quad (59)$$

$$\xi_1^\pm = \nu \left(\frac{\zeta'_r}{\omega} - \frac{b'_\pm}{b_\pm} \right) \Big|_{u^*} \frac{u^* - u}{(b_\pm^* t_0)^\Delta}. \quad (60)$$

F. Universal amplitude ratios

Even though the leading amplitude and subsequent Wegner expansion coefficients are fluid-dependent, certain combination ratios of these amplitudes are universal. From the equations for the first Wegner amplitudes of the specific heat, susceptibility, coexistence curve, and correlation length, one notices that the system-dependent part, $(u - u^*)/(b_\pm^* t_0)^\Delta$, is the same in every expression. Therefore the ratio of any of these first Wegner amplitudes is universal based on the MSR ϕ^4 model. These universal ratios have been given for the specific heat in ref. [4], [Eqs. (63), (64), and (68)]. In this paper we derive the other universal ratios based on the MSR ϕ^4 model. From Eqs. (32) and (33), one has the universal amplitude ratios for susceptibility,

$$\frac{\Gamma_0^+}{\Gamma_0^-} = \left(\frac{b_+^*}{b_-^*} \right)^\gamma \frac{f_-(u^*)}{f_+(u^*)} = 4.94, \quad (61)$$

$$\frac{\Gamma_1^+}{\Gamma_1^-} = \left(\frac{b_-^*}{b_+^*} \right)^\Delta \left. \frac{\gamma \frac{\zeta'_+}{\omega} - \gamma \frac{b'_+}{b_+} + \frac{\zeta'_\phi}{\omega} + \frac{f'_+}{f_+}}{\gamma \frac{\zeta'_-}{\omega} - \gamma \frac{b'_-}{b_-} + \frac{\zeta'_\phi}{\omega} + \frac{f'_-}{f_-}} \right|_{u^*} = 0.228. \quad (62)$$

From Eqs. (45) and (46), one obtains the universal amplitude ratios for specific heat,

$$\frac{A_0^+}{A_0^-} = \left(\frac{b_+^*}{b_-^*} \right)^\alpha \frac{4\nu B^* + \alpha F_+^*}{4\nu B^* + \alpha F_-^*} = 0.535, \quad (63)$$

$$\frac{A_1^+}{A_1^-} = 1.07. \quad (64)$$

Use of the scaling relation $\alpha + 2\beta + \gamma = 2$ and the combination of Eqs. (32), (45), and (54) leads to a universal ratio

$$\begin{aligned} R_c &= \frac{\alpha A_0^+ \Gamma_0^+}{B_0^2} \quad (65) \\ &= \frac{\alpha C_0 \chi_0 (F_+^* - A^*) (b_+^* t_0)^{\alpha+\gamma}}{\phi_0^2 (b_-^* t_0)^{-2\beta} f_\phi^* f_+^*} \\ &= \frac{\alpha (b_+^*)^{\alpha+\gamma} (b_-^*)^{-2\beta} (F_+^* - A^*)}{4 f_\phi^* f_+^*} = 0.0580. \end{aligned}$$

From Eqs. (59) and (60), the universal amplitude ratios for the correlation length are,

$$\frac{\xi_0^+}{\xi_0^-} = \left(\frac{b_+^*}{b_-^*} \right)^\nu = 1.42, \quad (66)$$

$$\frac{\xi_1^+}{\xi_1^-} = \left(\frac{b_-^*}{b_+^*} \right)^\Delta \left. \frac{\frac{\zeta'_+}{\omega} - \frac{b'_+}{b_+}}{\frac{\zeta'_-}{\omega} - \frac{b'_-}{b_-}} \right|_{u^*} = 1.10. \quad (67)$$

From Eqs. (45) and (59), one has the universal relation between the amplitude of specific heat and correlation length

$$\begin{aligned} \alpha A_0^\pm (\xi_0^\pm)^3 &= \mu^{-3} C_0 (b_\pm^* t_0)^{\alpha+3\nu} (4\nu B^* + \alpha F_\pm^*) \\ &= \frac{1}{16\pi} (b_\pm^*)^2 (4\nu B^* + \alpha F_\pm^*) \\ &= \begin{cases} 0.0206 & (T > T_c) \\ 0.0134 & (T < T_c) \end{cases}, \quad (68) \end{aligned}$$

where the scaling relation $\alpha + 3\nu = 2$ has been used. Equation (68) is identical to Eq. (S4.22) of ref.[6]. The evaluation of the right-hand side uses the constants given in Appendix A. A natural extension of Eq. (68) is the universal relation between specific heat and the correlation length throughout the crossover region. Using Eqs. (10), (20), and (42), and the scaling relation $\alpha + 3\nu = 2$, one has

$$C_\phi^\pm \xi_\pm^3 = \frac{b_\pm^2(l) K_\pm(l)}{16\pi |t|^2}. \quad (69)$$

TABLE I: The values of various universal amplitude ratios. The calculation for this work uses the values of the amplitude functions at the fixed point u^* given in Table IV and the values of the critical exponents given by Guida and Zinn-Justin [3].

Amplitude ratios	This work	B and B ^a	F and Z ^b
Γ_0^+/Γ_0^-	4.94	4.79 ± 0.10	4.95 ± 0.15
A_0^+/A_0^-	0.535	0.537 ± 0.019	0.523 ± 0.009
ξ_0^+/ξ_0^-	1.42		1.89 ± 0.015
R_c	0.0580	0.0574 ± 0.0020	0.0581 ± 0.0010
$\alpha A_0^+ (\xi_0^+)^3$	0.0206	0.0196 ± 0.0001	0.0188 ± 0.00015
$\alpha A_0^- (\xi_0^-)^3$	0.0134		0.0053 ± 0.00025
Γ_1^+/Γ_1^-	0.228	0.215 ± 0.029	
A_1^+/A_1^-	1.07	1.36 ± 0.47	
ξ_1^+/ξ_1^-	1.10		
B_1/Γ_1^+	0.76	0.40 ± 0.35	

^aBagnuls and Bervillier [5]

^bFisher and Zinn [9]

Since there is no fluid-dependent parameters appearing on the right hand side of Eq. (69), the product of the critical specific heat and the cubic of the correlation length is universal for any given temperature throughout the crossover region.

Table I lists the various universal amplitude ratios derived from the minimal-subtraction renormalization scheme, Bagnuls and Bervillier's massive-renormalization scheme [5], and other methods, such as ϵ -expansion, summarized by Fisher and Zinn [9]. The values given by Bagnuls and Bervillier are closely matched to the values given by Guida and Zinn-Justin [3] after the readjustment of the Borel resummation criteria [5]. Noticeable differences exist in Table I among various theories. In attempting to explain these differences, two factors are important to note. First, we are unable to evaluate the uncertainties of the universal ratios since the uncertainties of the universal ratios since the uncertainties on the Borel resummations at the fixed point u^* for most of the amplitude functions were not given in previous studies. Secondly, Eqs. (33), (46), and (60) use the derivatives of Eqs. (12), (13), (18), (24), (37), and (39) which could have sizable systematic uncertainties. These equations were only obtained from two-loop calculations and extrapolated to the five-loop fixed point values with adjustable constants. Hence it is desirable to have these derivatives calculated at the fixed point with Borel resummations. Then the extrapolation coefficients can be more accurately reconstructed, leading to the estimates of the first Wegner coefficients with less uncertainties.

III. FIT TO EXPERIMENTAL MEASUREMENTS

The expressions within the MSR model are parametric for susceptibility, specific heat, coexistence curve, and correlation length along the critical isochore and coexistence curve. We made a variable change of $l = \exp(-x)$ in solving those expressions numerically. x was discretized with 1000 data points over the range of $-\infty < x < \infty$ to obtain the solution for $u(x)$ over the range of $0 \leq u(x) \leq u^*$. For each thermal property versus reduced temperature, say χ_+ vs t , 1000 data points were calculated for a look-up table of $\chi_+(x_i)$ vs $t(x_i)$ with $i = 1, \dots, 1000$. The intended property was then obtained for a given reduced temperature t using a cubic spline.

This MSR model has three system dependent parameters, u , μ , and a which fix the scales for $u(l)$, $\xi(l)$, and $t(l)$ in Eqs. 9, 10, and 19. Here $u(l)$, $\xi(l)$, and $t(l)$ are defined implicitly as functions of the RG flow parameter l . Since l is eliminated in final solution, it is clear that one of the three amplitudes is redundant. This should not be mistaken as a minimal number of three fitting parameters for a complete equation-of-state while we only fit the thermal properties along the critical isochore and coexistence curve. In this paper $\{\mu, a\}$ are chosen as fitting parameters for a prefixed u because their combination only appears in the amplitude of the parametric expressions, such as t_0 , χ_0 , C_0 , etc. The u value is chosen based on the consideration that the expressions for the first Wegner amplitudes were derived by ignoring higher order terms in $[u(l) - u^*]$. Therefore an accurate determination of the first Wegner amplitudes requires u to be close to u^* .

Besides $\{\mu, a\}$, the critical temperature can also be a fitting parameter. Another adjustable parameter is required for the analytic background contribution to specific heat. In fitting the experimental data, y_{expt} , to theory, we minimize

$$\chi^2 = \sum_{i=1}^N \left(\frac{y_{\text{expt}}(x_i) - y_{\text{theory}}(x_i, \vec{a})}{\sigma_i} \right)^2. \quad (70)$$

Here \vec{a} is an array of fitting parameters with the standard error σ given by

$$\sigma^2 = \sigma_y^2 + \left(\frac{\partial y}{\partial x} \right)_{\vec{a}}^2 \sigma_x^2. \quad (71)$$

The partial derivative in Eq. (71) is evaluated numerically in each fitting iteration. The x in Eq. (70) is temperature. In our experiment, the sample temperature was determined from a resistance measurement having an approximately 10 μK uncertainty, i.e. $\sigma_x = 1 \times 10^{-5}$ K. In fitting the measurements of

isothermal susceptibility and specific heat, we assign $\sigma_y = k \times y/100$, assuming a $k\%$ uncertainty in the measurement.

The goodness of a fit is characterized by the value

$$\chi_\nu^2 = \frac{\chi^2}{N - M}, \quad (72)$$

where N is the number of data points and M is the number of fitting parameters.

All the experimentally measured quantities were made dimensionless by expressing them in units of appropriate combinations of the ^3He critical temperature $T_c = 3.315$ K, critical density $\rho_c = 0.04145\text{g/cm}^3$, and critical pressure $P_c = 1.14$ Pascal.

The experimental susceptibility, $\chi_T = \rho(\partial\rho/\partial P)_T$, is scaled by ρ_c^2/P_c to obtain the dimensionless susceptibility, $\chi_T^* \equiv \chi_T P_c / \rho_c^2$. The physical order parameter, $\Delta\rho \equiv \rho/\rho_c - 1$ is already dimensionless. The measured heat capacity had units of $[C] = \text{J/K}$. It was then divided by the fluid volume to have a unit of $[\rho C_V] = \text{J}/(\text{cm}^3 \text{K})$. Since the energy unit is $[J] = [P][V]$, a dimensionless specific heat was obtained as $C_V^* \equiv \rho C_V T_c / P_c$ with $P_c/T_c = 0.03463\text{J}/(\text{cm}^3 \text{K})$.

The critical specific heat C_ϕ^\pm per unit volume (divided by Boltzmann's constant k_B) near T_c is given by Eq. (42). The volume scaling factor is $v_0 = k_B T_c / P_c$, thus the length scaling factor is

$$l_0 = v_0^{1/3} = (k_B T_c / P_c)^{1/3}. \quad (73)$$

For ^3He , one has $l_0 = 7.36 \text{ \AA}$. It is assumed that μ is dimensionless in the MSR ϕ^4 model expressions with l_0^{-1} being the scaling factor, one defines $\xi^* \equiv \xi/l_0$.

A. Fit to susceptibility measurements

The susceptibility along the critical isochore ($\rho = \rho_c$) was determined using PVT measurements from both sides around ρ_c . The susceptibility along the coexistence curve was also determined using PVT measurements. For example, χ_T^{liq} was obtained from PVT measurements for $\rho > \rho_{coex}^{liq}$ and χ_T^{vap} was obtained from $\rho < \rho_{coex}^{vap}$.

Since χ_T^* varies sharply as $\rho \rightarrow \rho_c$ and $\rho \rightarrow \rho_{coex}$, the dominating uncertainty in χ_T^* comes from the uncertainty in locating either ρ_c for measurements above T_c and $\rho = \rho_{coex}$ for measurements below T_c . Above T_c , the inflection point was well confined by the data from the both sides of ρ_c . Below T_c , $\rho = \rho_{coex}$ was determined from a kink in P versus ρ curve. However, this kink becomes less pronounced as $T \rightarrow T_c$. Based on our observation, we assigned the susceptibility uncertain-

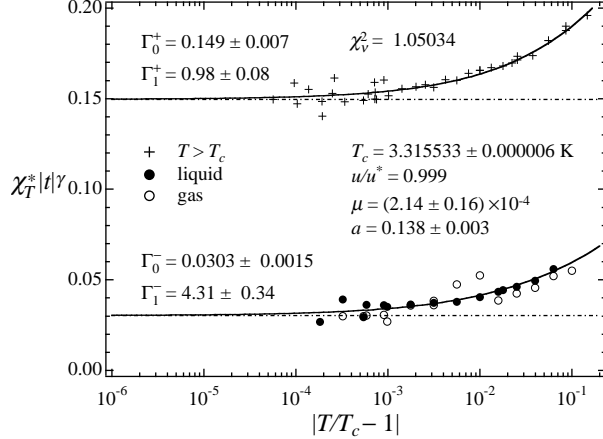


FIG. 1: Fit of MSR ϕ^4 model to ^3He susceptibility measurements for both $T > T_c$ and $T < T_c$. u/u^* is fixed to be 0.999, while T_c , μ , and a were adjusted. The solid line is the best fit. The dot-dashed straight lines represent the asymptotic predictions from the fit.

ties to be $\sigma_{\chi_T}(T > T_c) = 0.02\chi_T(T > T_c)$ and $\sigma_{\chi_T}(T < T_c) = 0.1\chi_T(T < T_c)$.

The results of fitting the susceptibility measurements for both $T > T_c$ and $T < T_c$ to the MSR expression in Eq. (26) is shown in Fig. 1. The susceptibility was scaled by $|t|^\gamma$ in order to provide a more sensitive representation of the crossover behavior and the fitting quality. The dot-dashed straight lines represent the asymptotic predictions from the MSR fit. The uncertainties in the amplitudes were deduced from the uncertainties of μ and a in the fit.

Figure 2 shows χ_ν^2 and $\{\mu, a\}$ versus $(1 - u/u^*)$. It is interesting to see that the goodness of the fit remains unchanged over a wide range of $(1 - u/u^*)$. This verifies that only two out of the three fluid-dependent parameters are relevant fitting parameters. We note here that no improvement in χ_ν^2 was made within scatters when u/u^* was also free to be adjusted in the fit.

Also shown in Fig. 2 are the calculated Γ_0^+ and Γ_1^+ versus $(1 - u/u^*)$. Γ_1^+ reaches a plateau for $(1 - u/u^*) \leq 4 \times 10^{-3}$ since the analytical expression for Γ_1^+ was derived by ignoring $O((1 - u/u^*)^2)$ or higher order terms. Therefore in this work we fix the value of $u/u^* = 0.999$.

Furthermore, $\mu \propto (1 - u/u^*)^{2\nu}$ and $a \propto (1 - u/u^*)^{4\nu-2}$ for $(1 - u/u^*) < 0.1$ implies a strong correlation between μ and a when susceptibility is chosen in fitting the MSR ϕ^4 theory to experimental data. The above power-law dependence of μ and a on $(1 - u/u^*)$ comes from the fact that Γ_1^+ is nearly a constant for $(1 - u/u^*) < 1 \times 10^{-2}$. Thus from Eq. (33) $t_0 \approx \mu^2/a \propto (1 - u/u^*)^{1/\Delta} \approx (1 - u/u^*)^2$.

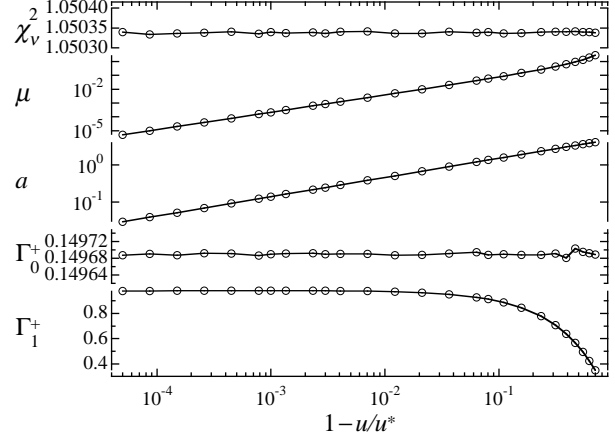


FIG. 2: The susceptibility fitting quality χ_ν^2 , parameters μ and a , and the resultant critical amplitudes versus fixed u/u^* . Γ_0^+ and Γ_1^+ were calculated using Eqs. (32) and (33) for each set of $\{u, \mu, a\}$ from the fit.

B. Fit to specific heat measurements

The specific heat, C_V , near the ^3He critical point was measured using a heat pulse method. The temperature change could be measured very accurately using a magnetic susceptibility thermometer with 1 nK resolution. For $T > T_c$, temperature equilibration was very fast due to the ‘‘piston effect’’ [14], and the uncertainty in the measured C_V was $\sim 1\%$, i.e. $\sigma_{C_V}(T > T_c) = 0.01C_V(T > T_c)$. For $T < T_c$, equilibration underwent critical slowing down as the fluid approached T_c . The slowing-down was due to the mass transfer at the meniscus between liquid and vapor. Since the sample cell was not perfectly adiabatic due to its mechanical support and electrical wires, there was some heat loss from the cell to the surrounding during the long equilibration. The uncertainty in measuring C_V was typically 5%, i.e. $\sigma_{C_V}(T < T_c) = 0.05C_V(T < T_c)$.

In fitting C_V measurements to the MSR ϕ^4 model, an additional adjustable parameter, C_B , appears in Eq. (42). By treating C_B as a constant within a small reduced temperature range around T_c , the true crossover behavior described by the MSR ϕ^4 model can be revealed. Figure 3 shows a fit of the C_V measurements for both $T > T_c$ and $T < T_c$ to the MSR expression in Eq. (42). The fit was limited to the reduced temperature range $|t| \leq 2 \times 10^{-2}$ as indicated by an arrow in the figure. The agreement between the experimental measurements and the theory is good. The uncertainties in the critical amplitudes and fluctuation-induced background

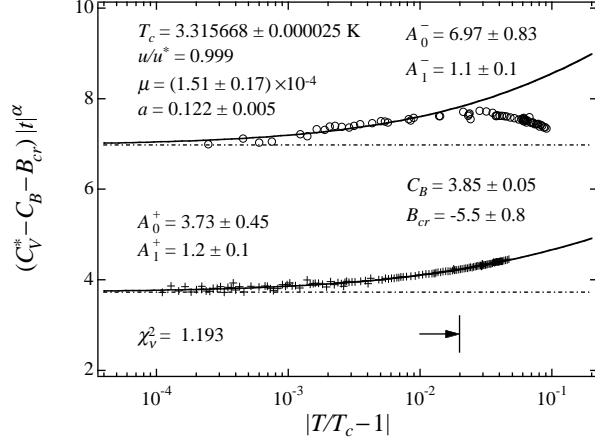


FIG. 3: The dimensionless specific heat at constant volume versus reduced temperature. The symbols represent the experimental measurements. The solid line is the best fit. The dot-dashed straight lines represent the asymptotic predictions from the fit. The arrow indicates the fitting range $|t| \leq 2 \times 10^{-2}$.

were error-propagated from the uncertainties of μ and a .

The fluctuation-induced background specific heat, B_{cr} , was calculated from Eq. (C16) in Appendix C. Its absolute value is close to that of C_B . As a result, the combined background specific heat is close to zero for ${}^3\text{He}$ as first demonstrated experimentally by Brown and Meyer [15].

C. Fit to Coexistence Curve Measurements

The best data for the ${}^3\text{He}$ coexistence curve was compiled in a recent paper by Luijten and Meyer [12]. We apply the MSR ϕ^4 model to the coexistence curve using these data as shown in Fig. 4. The fit was limited to the range $6 \times 10^{-4} \geq |t| \geq 4 \times 10^{-2}$. The lower bound was so chosen since the measurements were affected by the gravity effect for $|t| < 6 \times 10^{-4}$ due to a large cell height (4.3 mm) used in that experiment [16]. The upper bound was so chosen since the ϕ^4 model was developed for critical phenomena and did not include analytic behavior associated with a system approaching absolute zero temperature. The standard deviation for $|\Delta\rho_{L,V}|$ was approximated based on the percentile deviation in Fig. 5 of ref. [16], namely 1% at $|t| = 6 \times 10^{-4}$ and 0.2% at $|t| > 1 \times 10^{-2}$. The standard deviation for reduced temperature was $\delta T = 1 \times 10^{-5}\text{K}$ divided by $T_c = 3.3155\text{K}$.

The solid line in the figure represents the best fit with only $\{\mu, a\}$ adjusted. The predicted $B_0 = 1.02$ is consistent with the reported $B_0 = 1.02$ in ref. [12].

The agreement between the model calculation and the experimental data is satisfactory over the fitting range. The systematic difference between the MSR ϕ^4 model calculation and the measurements over the fitting range also exists from other theoretical model calculations [12].

The systematic deviation between the MSR ϕ^4 model calculation and the experimental data over the fitting range may be due to the fact that there was no proper background contribution included in the analysis. We attempt in this paper to include the effect of the order parameter saturation as a possible background contribution. The saturation of order parameter at absolute zero temperature has been studied by Povodyrev *et al.* [17] for an ideal Ising model. We propose an empirical expression that is consistent with that study for the limiting behavior at $|t| = 1$. Not only does the order parameter saturate to a constant value but its slope also approaches zero at $|t| = 1$. In the case of the liquid-vapor system where the physical order parameter is the normalized density difference from the critical value, the saturation value is also unity. Our empirical expression, satisfying this limiting behavior, is

$$\Delta\rho_{L,V} = \langle\phi\rangle \exp(-|t|/t_1) \pm b_2 [1 - \exp(-|t|/t_2)]. \quad (74)$$

In fitting the expression in Eq. (74) to the experimental data, only t_1 is adjusted while t_2 and b_2 are solved for a given t_1 through the constraints $\Delta\rho_{L,V} = \pm 1$ and $d\Delta\rho_{L,V}/dt = 0$ at $|t| = 1$. Near the critical point, the exponential damping of the first and second terms on the right hand side of Eq. (74) are negligibly small as evidenced by the large best fit values $t_1 = 1.56$, $t_2 = 4.55$, and $b_2 = 0.921$. As it can be seen in Fig. 4, the addition of the saturation background (dashed line) only slightly improves the systematic difference between the theory and the experimental data for $|t| < 4 \times 10^{-2}$ although it represents the data quite well for $|t| > 4 \times 10^{-2}$.

D. χ_T , C_V , and $|\Delta\rho_{L,V}|$ joint fit

The good individual fit of the MSR ϕ^4 model to isothermal susceptibility χ_T , specific heat C_V , and coexistence curve $|\Delta\rho_{L,V}|$ has been demonstrated. A joint fit of all the three thermal properties leads to a complete test of the MSR ϕ^4 model with a minimum set of the parameters, $\{\mu, a, T_c, C_B\}$. Here no order parameter saturation was included since its correction over the fitting range was small.

To make sure that no particular measurement dominates the joint fit, a proper weighting is needed to balance uneven numbers of the experimental data.

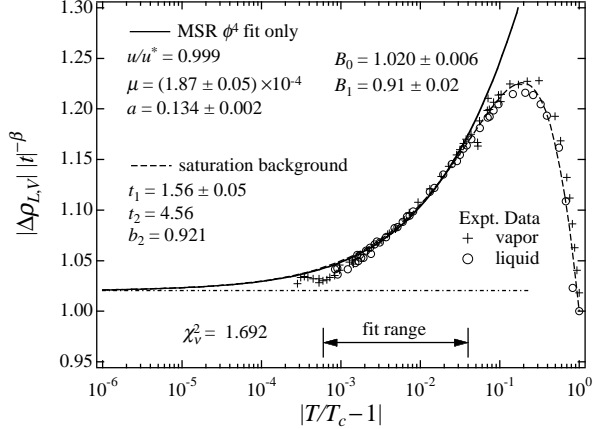


FIG. 4: Application of the MSR ϕ^4 model to the data of the ^3He coexistence curve. The solid line is the best fit with $\{\mu, a\}$ adjusted. The dashed line includes the empirical background contribution with $\{\mu, a\}$ fixed from the fit without the background. The dot-dashed straight line represents the asymptotic prediction from the fit.

We chose the following weighting in order to normalize the χ^2 by the number of data points,

$$\chi^2 = \frac{N}{3} \left(\frac{\chi_{\chi_T^*}^2}{N_{\chi_T^*}} + \frac{\chi_{C_V^*}^2}{N_{C_V^*}} + \frac{\chi_{\Delta\rho_{L,V}}^2}{N_{\Delta\rho_{L,V}}} \right) \quad (75)$$

where $N = N_{\chi_T^*} + N_{C_V^*} + N_{\Delta\rho_{L,V}}$. In the joint fit, χ_T^* and C_V^* were fit against temperature T while $|\Delta\rho_{L,V}|$ was fit against reduced temperature $|t|$, and μ, a, C_B , and T_c were adjusted. The joint fit results are shown in Fig. 5 and Table II. We note that in the joint fit the uncertainties in μ and a are much smaller than in the individual fits even though the overall goodness of fit is worse in the joint fit. These improved uncertainties in μ and a also lead to the improved uncertainties in the critical amplitudes and the fluctuation-induced background for specific heat.

Shown as dashed lines in Fig. 5 are the Wegner expansions to first order with the critical amplitudes, Γ_0^\pm and Γ_1^\pm , A_0^\pm and A_1^\pm , B_0 and B_1 , calculated from the MSR ϕ^4 model. Bagnuls and Bervillier [2] have argued that the validity range of any ϕ^4 model is upper-bounded when the difference between the calculations of the model and the Wegner expansion to first order becomes significant. Based on this argument, the validity range of the MSR ϕ^4 model is $|t| \simeq 1 \times 10^{-2}$. However, it is interesting to see that the MSR ϕ^4 model provides a good fit beyond $|t| = 1 \times 10^{-2}$ to the experimental measurements of the isothermal susceptibility both above and below T_c and the specific heat above T_c .

Close to T_c , the susceptibility data for $T > T_c$ and the specific heat data for both $T < T_c$ and $T > T_c$ deviate slightly from the theoretical pre-

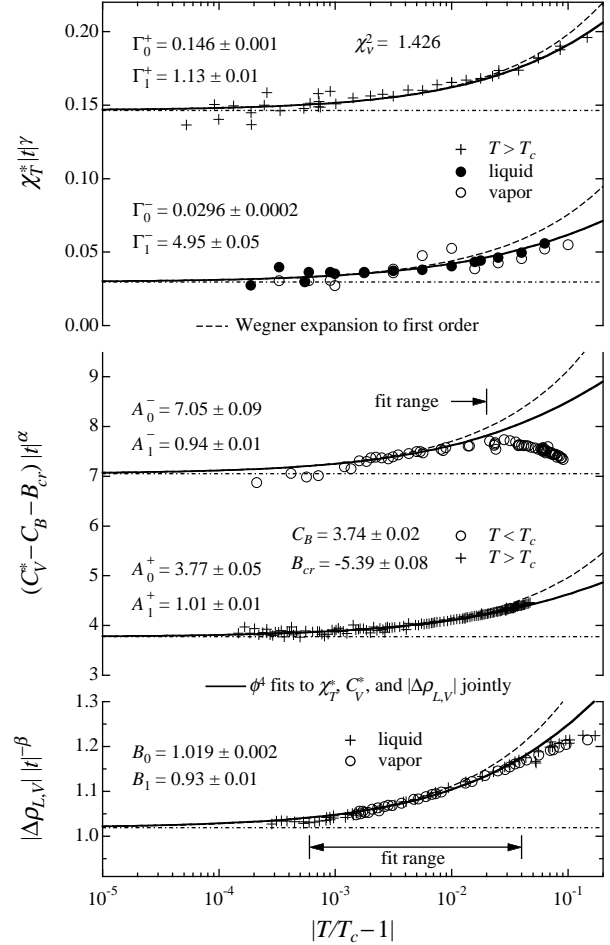


FIG. 5: A joint fit (solid lines) to susceptibility, specific heat, and coexistence curve. The fit used all the shown χ_T^* data and the data of C_V^* and $|\Delta\rho_{L,V}|$ over the indicated range. The dashed lines are the Wegner expansion to first order with the listed amplitudes in Table II. The dot-dashed straight lines represent the asymptotic predictions from the fit.

diction. These deviations can be attributed to a gravity-induced density stratification. Since the specific heat was measured as an average of the whole cell while the susceptibility was measured locally across a density sensor, there was a stronger gravity effect in the measured C_V than χ_T . The gravity effect on $\chi_T(T < T_c)$ is about a factor of five smaller than that on $\chi_T(T > T_c)$ because of the difference in χ_T magnitudes. When T_c is used as an adjustable parameter, the individual fits of susceptibility and specific heat tend to skew T_c such that the difference between the experimental measurements and theoretical prediction is minimized because of the shift in reduced temperature for the measurements. The T_c determined from the fits of the specific heat (Fig. 3) and susceptibility data (Fig. 1)

TABLE II: The dimensionless system-dependent parameters for ${}^3\text{He}$. The adjustable parameters are obtained from the joint fit of the ϕ^4 model to the measured χ_T^* , C_V^* , and $|\Delta\rho_{L,V}|$ data of ${}^3\text{He}$.

T_c (fit)	3.315546 ± 0.000005
u/u^* (fixed)	0.999
$\mu \times 10^4$ (fit)	1.82 ± 0.02
a (fit)	0.132 ± 0.001
C_B (fit)	3.74 ± 0.02
Γ_0^+	0.146 ± 0.001
Γ_0^-	0.0296 ± 0.0002
Γ_1^+	1.13 ± 0.01
Γ_1^-	4.95 ± 0.05
A_0^+	3.77 ± 0.05
A_0^-	7.05 ± 0.09
A_1^+	1.01 ± 0.01
A_1^-	0.94 ± 0.01
B_{cr}	-5.39 ± 0.08
B_0	1.019 ± 0.002
B_1	0.93 ± 0.01
ξ_0^+	0.368 ± 0.002
ξ_1^+	0.732 ± 0.007
ξ_0^-	0.259 ± 0.001
ξ_1^-	0.665 ± 0.006

tends to be higher and lower, respectively, than it should be. This tendency was approximately cancelled out in the joint fit shown in Fig. 5. The slight gravity effect on the experimental measurements for $1 \times 10^{-4} < |t| < 6 \times 10^{-4}$ can be clearly seen in Fig. 5.

We mention that in ref. [18] earlier measurements of the susceptibility of ${}^3\text{He}$, both above and below T_c , were compared with the present data. Also in Table I of that reference, the amplitudes of susceptibility and coexistence curve data and their ratios, such as Γ_1^+/B_1 and Γ_1^+/Γ_1^- , obtained from individual fits, were presented.

E. Predictions for correlation length and light scattering intensity

By using u/u^* , μ , and a given in Table II, the dimensionless correlation length can be calculated for any given $|t|$ using Eq. (56). Figure 6 shows the dimensionless correlation length versus t calculated from the MSR ϕ^4 model for ${}^3\text{He}$. The length scale to recover the dimensional ξ_0 is l_0 , given by Eq. (73). Thus one has a dimensional $\xi_0 = \xi_0^* l_0 = 2.71 \text{ \AA}$. This value can be directly compared with $\xi_0 = 2.6 \text{ \AA}$ measured in an acoustic experiment ref. [19]. Considering that the experimental ξ_0 had 10% uncertainty, the agreement is very good.

The correlation length can also be determined

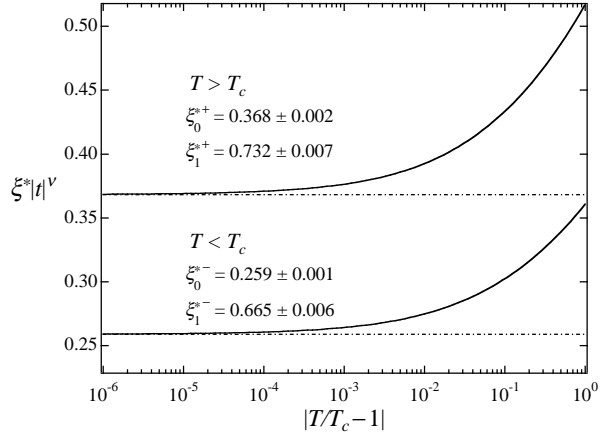


FIG. 6: The dimensionless correlation length versus reduced temperature calculated from the MSR ϕ^4 model for ${}^3\text{He}$. The dot-dashed straight lines represent the asymptotic predictions from the fit.

from a light scattering experiment. Miura, Meyer, and Ikushima measured the intensity of scattered light of ${}^3\text{He}$ fluid near its critical point [13]. The intensity scattered per unit beam length per unit solid angle in the fluid, I , is given by

$$I = I_0 A \chi_T \sin^2 \phi g(k\xi), \quad (76)$$

where I_0 is the beam intensity in the scattering region, ϕ is the angle between the electric field of the incident light and the wave vector of the scattered light, χ_T is the susceptibility, and $A = \pi^2 k_B T (\partial n^2 / \partial \rho)_T^2 / \lambda_0^4$. Here n is the index of refraction of the fluid, and λ_0 is the vacuum wavelength of the incident light. The function $g(k\xi)$ is, for $k\xi \leq 10$, very accurately given by the Ornstein-Zernike approximation $(1 + k^2 \xi^2)^{-1 + \eta/2}$, where k is the scattering wave vector, ξ is the correlation length, and η is the critical exponent of the fluctuation correlation at the critical point. In ref. [13], $k = 5.64 \times 10^4 \text{ cm}^{-1}$. At $t = 1 \times 10^{-6}$, the value of correlation length can be estimated from $\xi = 2.71 \text{ \AA} t^{-0.63} = 1.63 \times 10^{-4} \text{ cm}$, hence the condition $k\xi(t = 1 \times 10^{-6}) = 9.2 \leq 10$ was satisfied for $t \geq 1 \times 10^{-6}$. Since $B = I_0 A \sin^2 \phi$ is essentially a constant for the experimental condition, one can use the knowledge of χ_T and ξ , based on the MSR ϕ^4 model, to fit experimental data of the scattered intensity, with B as an adjustable parameter. As it can be seen in Fig. 7, the agreement between the experimental data and theoretical calculation is reasonably good.

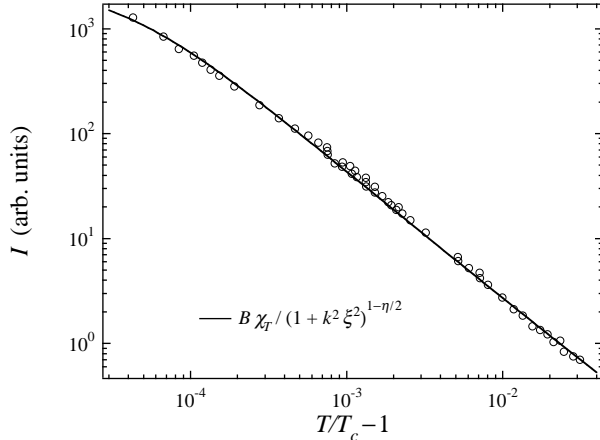


FIG. 7: The intensity of light scattered by ^3He versus reduced temperature. The theoretical calculated I , using the MSR ϕ^4 model, is adjusted with a constant amplitude for $I_0 A$ while u/u^* , μ , and a were fixed from the values given in Table II.

IV. DISCUSSION

In this paper we have used parametric expressions to calculate the isothermal susceptibility, specific heat, coexistence curve, and correlation length along the critical isochore and coexistence curve from the asymptotic region to the crossover region. All the critical leading amplitude ratios were contained in the model as listed in Table I. Using only two adjustable parameters in these theoretical expressions for the critical contributions, we fit the theory to recently obtained experimental data for the isothermal susceptibility, specific heat, and early experimental data of the coexistence curve and light scattering intensity. The agreement between the theory and experimental measurements is good.

Further improvements to the minimal renormalization scheme are desired, especially the five-loop Borel resummations throughout the whole range of $0 \leq u \leq u^*$. More accurate Borel resummations at the fixed point should also lead to improved calculations of $\zeta_\phi(u^*)$ and $\zeta_r(u^*)$ so that the resultant critical exponents can be compared with other published values (see Appendix A). Theoretical insights on non-critical contributions are also needed in order to formulate more accurate analytical expressions for the background contributions.

While the present minimal subtraction renormalization model describes quite well to experimental measurements along the critical isochore and coexistence curve, it is not as yet a model for a complete equation-of-state. Recently, Agayan *et al.* have developed a phenomenological crossover parametric model (CPM) equation-of-state that is also based

upon RG theory [20]. Within this model, the internal constants were adjusted such that the critical leading constants agreed with the values in the Fisher and Zinn column in Table I. This CPM model was developed to fit simple fluids as well as complex fluid systems that exhibit non-monotonic crossover behavior. This non-monotonic crossover behavior could be described by the CPM approach using a finite cut-off wavelength as an additional fitting parameter. However, in simple fluid systems, like ^3He , crossover behavior of different physical quantities can be well described within the framework of the field theoretical ϕ^4 model without the finite cut-off wavenumber.

NASA supported microgravity flight experiments [21, 22] (<http://miste.jpl.nasa.gov>), which are under preparation, will take experimental data of the susceptibility, specific heat, and coexistence curve in the asymptotic region. Combining these microgravity measurements in the asymptotic region with ground-based measurements in the crossover region should permit a rigorous test of the predictions of recent renormalization theories.

Acknowledgments

We are indebted to Dr. R. Haussmann and Prof. J. Rudnick for supporting the early development of this work and for many stimulating discussions. We are also grateful to Prof. H. Meyer for a critical reading of the manuscript and to Dr. M. Weilert for his contribution in performing the experiments. The research described in this paper was carried out at the Jet Propulsion Laboratory, California Institute of Technology, under contract with the National Aeronautics and Space Administration.

APPENDIX A: THE MSR ϕ^4 MODEL CONSTANTS

The field-theoretic functions, $\zeta_r(u)$, $\zeta_\phi(u)$, and $\beta_u(u)$, and the amplitude functions, $P_\pm(u)$, $Q(u)$, $f_\pm(u)$, $F_\pm(u)$, $A(u)$, and $B(u)$ are known up to five-loop order from expansions around $u = 0$. However, these expansions do not converge. To overcome this difficulty, these quantities were expanded to two-loop order and then extrapolation terms were added to have the functions agree with the calculations of high-order Borel resummations at the fixed point [1]. All these functions have at least one extrapolation term to match the function's value at the fixed point u^* ; some functions also have a second extrapolation term in order to match the value of its derivative at the fixed point. Listed in this appendix are the

values of these extrapolation coefficients, their origins, and recent improvements. The effects of these coefficient values on the critical exponents and the fitting quality in this work are discussed.

The extrapolation coefficients for the field-theoretic functions, $\zeta_r(u)$, $\zeta_\phi(u)$, and $\beta_u(u)$ in Eqs. (6), (7), (8) are $a_1 = 3075$, $a_2 = 30390$, $a_3 = 37.5$, $a_4 = 14.10$, and $a_5 = 31.85$. They are taken from Table 2 of ref.[1].

The fixed point value for $u^* = 0.040485$ is solved from the condition $\beta_u(u^*) = 0$ using the given values for a_4 and a_5 . The latest published u^* value for $n = 1$ is [4]

$$u^* = 0.0404 \pm 0.0003. \quad (\text{A1})$$

The asymptotic critical exponents are linked to the exponent functions ζ_r , ζ_ϕ , and β_u by

$$\eta = -\zeta_\phi(u^*) = -\zeta_\phi^* = 0.0367, \quad (\text{A2})$$

$$\nu = [2 - \zeta_r(u^*)]^{-1} = (2 - \zeta_r^*)^{-1} = 0.629, \quad (\text{A3})$$

$$\omega = \left. \frac{d\beta_u(u, \epsilon = 1)}{du} \right|_{u^*} = 0.797. \quad (\text{A4})$$

Once the critical exponents, η , ν , and ω are known, the remaining important critical exponents can be obtained from scaling using

$$\alpha = \frac{1 - 2\zeta_r^*}{2 - \zeta_r^*} = 0.112, \quad (\text{A5})$$

$$\beta = \frac{1 - \zeta_\phi^*}{2(2 - \zeta_r^*)} = 0.326, \quad (\text{A6})$$

$$\gamma = \frac{2 + \zeta_\phi^*}{2 - \zeta_r^*} = 1.235, \quad (\text{A7})$$

$$\Delta = \nu\omega = 0.502. \quad (\text{A8})$$

For $n = 1$, the latest theoretically calculated critical exponents given by Guida and Zinn-Justin [3] are,

$$\nu = 0.6304 \pm 0.0013, \quad (\text{A9})$$

$$\eta = 0.0335 \pm 0.0025, \quad (\text{A10})$$

$$\alpha = 0.109 \pm 0.004, \quad (\text{A11})$$

$$\beta = 0.3258 \pm 0.0014, \quad (\text{A12})$$

$$\gamma = 1.2396 \pm 0.0013, \quad (\text{A13})$$

$$\omega = 0.799 \pm 0.011, \quad (\text{A14})$$

$$\Delta = \omega\nu = 0.504 \pm 0.008, \quad (\text{A15})$$

A clear difference exists for the value of the critical exponent γ which warrants further efforts from the theoretical community for improvements in the MSR ϕ^4 model calculation.

The amplitude function $Q(u(l))$ for reduced temperature is expressed as

$$Q(u(l)) = 2 \int_{u^*}^{u(l)} du' \frac{P_+(u')}{\beta_u(u')} \exp \int_{u(l)}^{u'} du'' \frac{2 - \zeta_r(u'')}{\beta_u(u'')}. \quad (\text{A16})$$

At the fixed point u^* , there is an identity $\nu^{-1} = 2 - \zeta_r^*$ that simplifies Eq. (A16) and leads to

$$Q^* = 2\nu P_+^*. \quad (\text{A17})$$

Krause *et al.* [8] obtained the expression [Eq. (K_A28)]

$$\left. \frac{dQ}{du} \right|_{u^*} = \frac{2 \left. \frac{dP}{du} \right|_{u^*} + Q^* \left. \frac{d\zeta_r}{du} \right|_{u^*}}{\omega + \nu^{-1}}, \quad (\text{A18})$$

with $\omega = d\beta_u/du|_{u^*}$. They also provided a one-loop expression for $P(u)$ using a higher-order approximation [Eq. (K3.2)] [8]

$$P_+(u) = 1 - 6u(1 + b_P u). \quad (\text{A19})$$

The latest calculation by Larin *et al.* [4] for $n = 1$ gives

$$P_+^* = 0.7568 \pm 0.0044. \quad (\text{A20})$$

If the theoretically calculated critical exponent ν for $n = 1$, given by Guida and Zinn-Justin [3], is used [4], one has

$$b_+ = 2\nu P_+^* = 0.9542 \pm 0.0059, \quad (\text{A21})$$

$$b_- = 3/2 - 2\nu P_+^* = 0.5458 \pm 0.0059. \quad (\text{A22})$$

For the extrapolation coefficients in the expression for $Q(u)$, Eq. (18), Krause *et al.* [8] determined $b_Q = 28.2$ and $c_Q = 7.66$ such that Eq. (A17) and (A18) were satisfied with the then calculated P_+^* . The values of the extrapolation coefficients $b_Q = 20.32$ and $c_Q = 6.24$ have been readjusted to agree with the new $Q(u^*) = 0.9542$. There is no value for $dP/du|_{u^*}$, so the new $dQ/du|_{u^*}$ has been fixed to its old value [8].

For the amplitude function $f_\pm(u)$ in the expression of the susceptibility, Eq. (26), $b_\chi = 9.68$ comes

TABLE III: The values of the various extrapolation coefficients for the amplitude functions in the MSR ϕ^4 model.

coefficient	value	appeared in
a_1	3075	$\zeta_r(u)$ for $Z_r(u)$
a_2	30390	$\zeta_r(u)$ for $Z_r(u)$
a_3	37.5	$\zeta_\phi(u)$ for $Z_\phi(u)$
a_4	14.10	$\beta_u(u)$ for $Z_u(u)Z_\phi(u)$
a_5	31.85	$\beta_u(u)$ for $Z_u(u)Z_\phi(u)$
b_Q	20.32	$Q(u)$ for $t(l)$
c_Q	6.24	$Q(u)$ for $t(l)$
b_χ	9.68	$f_+(u)$ for χ_T^+
d_χ	-11.18	$f_-(u)$ for χ_T^-
b_F	-5.0726	$F_+(u)$ for C_V^+
d_F	-4.6736	$F_-(u)$ for C_V^-
b_B	-20.6817	$B(u)$ for C_V^\pm
d_ϕ	0.702	$f_\phi(u)$ for $\Delta\rho_{L,V}$

from Table 1 of ref.[8] and $d_\chi = -11.18$ comes from Table 4 of ref. [7].

For the amplitude function in the expression of the specific heat, Eqs. (42), (36), and (37), the five-loop approximation with a Borel resummation gives [4]

$$u^* F_-(u^*) = 0.3687 \pm 0.0040. \quad (\text{A23})$$

By combining Eqs. (37)b, (A1), and (A23), the old interpolation coefficient, $d_F = -4.04$ (Table 4 of ref.[7]), becomes $d_F = -4.6736$. The latest five-loop calculation also gives [4]

$$u^*[F_-(u^*) - F_+(u^*)] = 0.4170 \pm 0.0036. \quad (\text{A24})$$

Using Eqs. (A23) and (A24), one has

$$-u^* F_+(u^*) = 0.0483 \pm 0.0076. \quad (\text{A25})$$

By combining Eqs. (37)a, (A1), and (A25), the old interpolation coefficient, $b_F = 5.04$ (Table 1 of ref.[8]), becomes $b_F = -5.07$.

We modify Eq. (39) to be

$$B(u) = \frac{1}{2} + 9(1 + b_B u)u^2 \quad (\text{A26})$$

with $b_B = -20.68$ in order to satisfy the five-loop Borel resummed results [Eq. (L2.34)] [4]

$$B(u^*) = 0.5024 \pm 0.001. \quad (\text{A27})$$

All the calculations use the value of u^* derived in this paper.

Table III lists the values of the various extrapolation coefficients for the amplitude functions in the MSR ϕ^4 model. Table IV lists the values of the various amplitude functions at the fixed point u^* .

Equations (20) and (26) provide a clear identification of the leading critical divergence and crossover

TABLE IV: The values of the various amplitude functions at the fixed point u^* . These values are used in the calculation of the leading critical amplitude ratios with $u^* = 0.040485$.

coefficient	value	appeared in
b_+^*	0.9542 ± 0.0059	$t(l)$ in Eq. (20)
b_-^*	0.5458 ± 0.0059	$t(l)$ in Eq. (20)
f_+^*	0.9767	Γ_0^+ for χ_T^+ in Eq. (32)
f_-^*	2.413	Γ_0^- for χ_T^- in Eq. (32)
$-u^* F_+^*$	0.0483 ± 0.0076	A_0^+ for C_ϕ^+ in Eq. (45)
$u^* F_-^*$	0.3687 ± 0.0040	A_0^- for C_ϕ^- in Eq. (45)
B^*	0.5024 ± 0.001	A^* for C_ϕ^\pm in Eq. (40)
f_ϕ^*	3.175	B_0 for $\Delta\rho_{L,V}$ in Eq. (54)

contribution in a multiplicative form. In the original expressions, the critical divergence is contained implicitly in the integrals of ζ_r and ζ_ϕ in Eqs. (15) and (23). The calculated $\zeta_r(u^*)$ and $\zeta_\phi(u^*)$ using Borel resummations at the fixed point lead to the critical exponents ν and η that are slightly different from the latest values given by Guida and Zinn-Justin. Because of the expressions in Eqs. (19) and (26), the critical exponent values given by Guida and Zinn-Justin are used for the leading divergence. The inconsistency is only in the crossover part in the integrands of $[\zeta_r(u) - \zeta_r(u^*)]$ and $[\zeta_\phi(u) - \zeta_\phi(u^*)]$ that go to zero as the fixed point is approached.

APPENDIX B: DERIVATION OF SUSCEPTIBILITY AMPLITUDES

Expressions for the Wegner expansion of the susceptibility will be derived in this Appendix that were not presented in previously published work. Multiplying Eq. (26) by Eq. (20) to the power γ yields

$$\chi_\pm |t|^\gamma = \chi_0 [b_\pm(l)t_0]^\gamma \frac{\exp[-F_\phi(l) - \gamma F_r(l)]}{f_\pm(l)}. \quad (\text{B1})$$

In order to expand the exponent functions, $F_r(u(l))$ and $F_\phi(u(l))$, based on Eqs. (22) and (28), one needs to expand first the function for the flow equation, $\beta_u(u(l))$, to the first order in $[u(l) - u^*]$,

$$\beta_u(u(l)) = \omega[u(l) - u^*] + O[(u(l) - u^*)^2], \quad (\text{B2})$$

where $\omega = d\beta_u/du|_{u^*}$ and $\beta_u(u^*) = 0$. Since $F_r(u^*) = 0$ and $F_\phi(u^*) = 0$, one obtains

$$\begin{aligned} F_r(u(l)) &= \lim_{u(l) \rightarrow u^*} \frac{\zeta_r(u(l)) - \zeta_r(u^*)}{\omega[u(l) - u^*]} [u(l) - u^*] \\ &+ O[(u(l) - u^*)^2] \\ &= \frac{\zeta_r'(u^*)}{\omega} [u(l) - u^*] + O[(u(l) - u^*)^2], \end{aligned} \quad (\text{B3})$$

$$\begin{aligned}
F_\phi(u(l)) &= \lim_{u(l) \rightarrow u^*} \frac{\zeta_\phi(u(l)) - \zeta_\phi(u^*)}{\omega[u(l) - u^*]} [u(l) - u^*] \\
&+ O[(u(l) - u^*)^2] \\
&= \frac{\zeta'_\phi(u^*)}{\omega} [u(l) - u^*] + O[(u(l) - u^*)^2],
\end{aligned} \tag{B4}$$

$$\begin{aligned}
f_\pm(u(l)) &= f_\pm(u^*) + f'_\pm(u^*)[u(l) - u^*] \\
&+ O[(u(l) - u^*)^2],
\end{aligned} \tag{B5}$$

$$\begin{aligned}
b_\pm(u(l)) &= b_\pm(u^*) + b'_\pm(u^*)[u(l) - u^*] \\
&+ O[(u(l) - u^*)^2].
\end{aligned} \tag{B6}$$

The expression $b_\pm(u(l))^\gamma \exp[-F_\phi(u(l)) - \gamma F_r(u(l))]/f_\pm(u(l))$ is then expanded in terms of $[u(l) - u^*]$, dropping the higher orders, to give

$$\begin{aligned}
\chi_\pm |t|^\gamma &= \frac{\chi_0 (b_\pm^* t_0)^\gamma}{f_\pm(u^*)} \times \\
&\left\{ 1 - \left[\gamma \left(\frac{\zeta'_r}{\omega} - \frac{b'_\pm}{b_\pm} \right) + \frac{\zeta'_\phi}{\omega} + \frac{f'_\pm}{f_\pm} \right] \Big|_{u^*} [u(l) - u^*] \right\}.
\end{aligned} \tag{B7}$$

The solution of the flow equation with $\beta_u(u)$ approximated by Eq. (B2) is

$$l^\omega = \frac{u(l) - u^*}{u - u^*}. \tag{B8}$$

By expressing l in terms of $|t|$ and dropping higher order terms, one has $l = |t|^\nu / (b_\pm^* t_0)^\nu$ and

$$\begin{aligned}
\chi_\pm |t|^\gamma &= \frac{\chi_0 (b_\pm^* t_0)^\gamma}{f_\pm(u^*)} \\
&\times \left[1 - \left(\gamma \frac{\zeta'_r}{\omega} - \gamma \frac{b'_\pm}{b_\pm} + \frac{\zeta'_\phi}{\omega} + \frac{f'_\pm}{f_\pm} \right) \Big|_{u^*} \right. \\
&\quad \left. \times \frac{u - u^*}{(b_\pm^* t_0)^{\nu\omega}} |t|^{\nu\omega} \right].
\end{aligned} \tag{B9}$$

Comparing Eq. (B9) to the standard Wegner expansion to the first term, see Eq. (31), one obtains the critical amplitudes of the susceptibility expressed analytically in Eqs. (32) and (33) with $\Delta = \nu\omega$.

APPENDIX C: DERIVATION OF SPECIFIC HEAT AMPLITUDES

A derivation of the critical amplitudes and constant background of the specific heat in the additive renormalization form will be given in this Appendix. This derivation is consistent with the one for susceptibility given above and is different from the one given by Schloms and Dohm [6].

First an expansion expression for the function $A(u(l))$ will be derived that is an approximate solution of Eq. (38). By expanding $B(u)$ and $\zeta_r(u)$ around u^* and omitting higher order terms beyond the linear term, Eq. (38) becomes

$$\begin{aligned}
l \frac{dA(l)}{dl} &= 4B(u^*) + 4B'(u^*)(u - u^*) \\
&+ [\alpha/\nu - 2\zeta'_r(u^*)(u - u^*)] A(l).
\end{aligned} \tag{C1}$$

Then Eq. (B8) is used to replace $(u - u^*)$ with l^ω , yielding

$$l \frac{dA(l)}{dl} = H + Yl^\omega + (G + Zl^\omega) A(l). \tag{C2}$$

where

$$H = 4B(u^*) \tag{C3}$$

$$G = \frac{\alpha}{\nu} \tag{C4}$$

$$Y = 4B'(u^*)(u - u^*) \tag{C5}$$

$$Z = -2\zeta'_r(u^*)(u - u^*). \tag{C6}$$

With a variable change of

$$v = \frac{l^\omega Z}{\omega}, \tag{C7}$$

Eq. (C2) becomes

$$v \frac{dA(v)}{dv} = \frac{H}{\omega} + \frac{Y}{Z} v + \left(\frac{G}{\omega} + v \right) A(v). \tag{C8}$$

The solution of Eq. (C8) is

$$\begin{aligned}
A(v) &= \exp(v) v^{\frac{G}{\omega}} \\
&\times \left[K_1 - \frac{H}{\omega} \Gamma \left(-\frac{G}{\omega}, v \right) - \frac{Y}{Z} \Gamma \left(1 - \frac{G}{\omega}, v \right) \right],
\end{aligned} \tag{C9}$$

where K_1 is a constant to be determined through the initial condition. Expanding Eq. (C9) in v and keeping only the linear terms of $l^{\alpha/\nu}$ and l^ω , one obtains

$$A(l) = A(u^*) + K_2(u - u^*)l^\omega + K_3 l^{\alpha/\nu}, \tag{C10}$$

where Eq. (40) is used for $A(u^*)$ and

$$\begin{aligned}
K_2 &= \frac{1}{(u - u^*)} \left[\frac{\nu Y}{\Delta - \alpha} + A^* \frac{\Delta}{\Delta - \alpha} \frac{Z}{\omega} \right] \\
&= \frac{2\nu}{\Delta - \alpha} [2B'(u^*) - A^* \zeta'_r(u^*)].
\end{aligned} \tag{C11}$$

K_3 in Eq. (C10) will be eliminated through initial condition at the reference point $l = 1$

$$K_3 = A_1 - A^* - K_2(u - u^*), \tag{C12}$$

where $A_1 \equiv A(l=1)$. Since A_1 has not been given as a fitting parameter, it is calculated from the numerical solution of Eq. (38) with $A(u=0) = -2$.

Substituting Eq. (C10) into Eq. (42), one has

$$\frac{C_\phi^\pm}{C_0} = -\exp[2F_r(l)]K_3 + \exp[2F_r(l)]l^{-\alpha/\nu} \times [F_\pm(l) - A^* - K_2(u - u^*)l^\omega]. \quad (\text{C13})$$

Replacing $l^{\alpha/\nu}$ in Eq. (C13) with t/t_0 from Eq. (20) leads to

$$\frac{C_\phi^\pm}{C_0} = -\exp[2F_r(l)]K_3 + \exp[(2 - \alpha)F_r(l)] [b_\pm(l)t_0]^\alpha |t|^{-\alpha} \times [F_\pm(l) - A^* - K_2(u - u^*)l^\omega]. \quad (\text{C14})$$

$F_r(l)$, $F_\pm(l)$, and $b_\pm(l)$ are expanded according to Eqs. (B3), (B5), and (B6) respectively. Higher order terms than $O[(u(l) - u^*)^2]$ or $O(l^{2\omega})$ are dropped in the expansion, and $(u(l) - u^*)$ is replaced using Eq. (B8). By using the approximation of $l^\omega = |t|^\Delta / (b_\pm^* t_0)^\Delta$, one finally has

$$\frac{C_\phi^\pm}{C_0} = -K_3 + (F_\pm^* - A^*) (b_\pm^* t_0)^\alpha |t|^{-\alpha} \times \left\{ 1 + \left[\frac{1}{F_\pm^* - A^*} (F_\pm' - K_2) + (2 - \alpha) \frac{\zeta_r'}{\omega} + \alpha \frac{b_\pm'}{b_\pm} \right] \Big|_{u^*} \right\} \times (u - u^*) \frac{|t|^\Delta}{(b_\pm^* t_0)^\Delta}. \quad (\text{C15})$$

By comparing Eq. (C15) to the standard Wegner expansion to the first term, see Eq. (44), one obtains the analytical expressions for the critical amplitudes of the specific heat given in Eqs. (45) and (46). The critical background specific heat is also identified as

$$B_{cr} = -C_0 K_3. \quad (\text{C16})$$

APPENDIX D: χ_T^* AND C_V^* EXPERIMENTAL MEASUREMENTS

We list in this Appendix the dimensionless experimental measurements of isothermal susceptibility, specific heat, and coexistence curve of ^3He . The ITS90 temperature standard was used in the following tables.

TABLE V: The dimensionless experimental measurements of the ^3He isothermal susceptibility χ_T^* . $T_c = 3.315545\text{K}$ was obtained from the joint fit of χ_T^* and C_V^* to the MSR ϕ^4 model. The index = 0, 19, 8 corresponds respectively to $T > T_c$, $\{T < T_c, \text{liquid}\}$, $\{T < T_c, \text{vapor}\}$.

T	$T/T_c - 1$	χ_T^*	index
3.3157200	5.288e-05	2.763e+04	0
3.3158500	9.209e-05	1.524e+04	0
3.3158770	1.002e-04	1.278e+04	0
3.3159900	1.343e-04	9.468e+03	0
3.3161700	1.886e-04	6.006e+03	0
3.3161770	1.907e-04	5.600e+03	0
3.3163600	2.459e-04	4.477e+03	0
3.3164000	2.580e-04	4.457e+03	0
3.3166570	3.355e-04	2.966e+03	0
3.3173270	5.376e-04	1.670e+03	0
3.3175600	6.078e-04	1.469e+03	0
3.3179100	7.134e-04	1.256e+03	0
3.3179170	7.155e-04	1.180e+03	0
3.3179400	7.225e-04	1.194e+03	0
3.3180170	7.457e-04	1.120e+03	0
3.3185400	9.034e-04	9.472e+02	0
3.3188970	1.011e-03	7.790e+02	0
3.3202400	1.416e-03	5.268e+02	0
3.3221970	2.006e-03	3.450e+02	0
3.3239900	2.547e-03	2.587e+02	0
3.3259870	3.149e-03	1.970e+02	0
3.3295500	4.224e-03	1.407e+02	0
3.3341869	5.623e-03	9.850e+01	0
3.3404500	7.512e-03	7.046e+01	0
3.3487469	1.001e-02	4.980e+01	0
3.3487600	1.002e-02	4.979e+01	0
3.3596699	1.331e-02	3.535e+01	0
3.3745467	1.780e-02	2.480e+01	0
3.3897402	2.238e-02	1.884e+01	0
3.3999300	2.545e-02	1.642e+01	0
3.3999967	2.547e-02	1.620e+01	0
3.4402800	3.762e-02	1.014e+01	0
3.4999362	5.561e-02	6.540e+00	0
3.4999899	5.563e-02	6.540e+00	0
3.6000160	8.580e-02	3.990e+00	0
3.6000502	8.581e-02	3.939e+00	0
3.8000406	1.461e-01	2.126e+00	0
3.3149265	-1.864e-04	1.151e+03	19
3.3144595	-3.273e-04	8.291e+02	19
3.3137295	-5.475e-04	3.271e+02	19
3.3135883	-5.901e-04	3.665e+02	19
3.3125410	-9.059e-04	2.145e+02	19
3.3122627	-9.899e-04	1.868e+02	19
3.3096911	-1.765e-03	9.418e+01	19
3.3050875	-3.154e-03	4.708e+01	19
3.2969714	-5.602e-03	2.344e+01	19
3.2824717	-9.975e-03	1.225e+01	19
3.2630551	-1.583e-02	7.408e+00	19
3.2566732	-1.776e-02	6.555e+00	19
3.2323114	-2.510e-02	4.455e+00	19
3.1836186	-3.979e-02	2.696e+00	19
3.1064086	-6.308e-02	1.717e+00	19
3.3144595	-3.273e-04	6.347e+02	8
3.3137295	-5.475e-04	3.326e+02	8

3.3135883	-5.901e-04	3.080e+02	8
3.3125410	-9.059e-04	1.820e+02	8
3.3122627	-9.899e-04	1.436e+02	8
3.3096911	-1.765e-03	9.300e+01	8
3.3051276	-3.142e-03	4.865e+01	8
3.3050875	-3.154e-03	4.533e+01	8
3.2969591	-5.606e-03	2.937e+01	8
3.2824590	-9.979e-03	1.586e+01	8
3.2630538	-1.583e-02	6.585e+00	8
3.2323290	-2.510e-02	4.100e+00	8
3.1836229	-3.979e-02	2.486e+00	8
3.1064148	-6.308e-02	1.600e+00	8
2.9840784	-9.997e-02	9.556e-01	8

3.237827	-2.344e-02	9.861
3.238887	-2.312e-02	9.836
3.245184	-2.122e-02	10.083
3.268550	-1.417e-02	10.452
3.269553	-1.387e-02	10.481
3.286051	-8.896e-03	11.023
3.287624	-8.421e-03	10.997
3.288580	-8.133e-03	11.091
3.296766	-5.664e-03	11.477
3.297686	-5.386e-03	11.591
3.298910	-5.017e-03	11.697
3.301335	-4.286e-03	11.856
3.304018	-3.477e-03	12.119
3.305181	-3.126e-03	12.209
3.306067	-2.859e-03	12.272
3.307219	-2.511e-03	12.498
3.308159	-2.228e-03	12.715
3.308833	-2.024e-03	12.833
3.309386	-1.858e-03	12.824
3.310214	-1.608e-03	13.081
3.311035	-1.360e-03	13.029
3.311577	-1.197e-03	13.314
3.313179	-7.135e-04	13.795
3.313675	-5.639e-04	14.128
3.314163	-4.167e-04	14.827
3.314846	-2.107e-04	15.637
3.316036	1.482e-04	8.389
3.316098	1.669e-04	8.595
3.316160	1.856e-04	8.159
3.316217	2.028e-04	8.289
3.316279	2.215e-04	7.875
3.316339	2.396e-04	7.907
3.316400	2.580e-04	7.823
3.316405	2.595e-04	7.992
3.316461	2.764e-04	7.654
3.316512	2.918e-04	7.572
3.316562	3.068e-04	7.689
3.316627	3.264e-04	7.617
3.316690	3.454e-04	7.643
3.316757	3.656e-04	7.274
3.316827	3.868e-04	7.473
3.316893	4.067e-04	7.407
3.316943	4.217e-04	7.611
3.316995	4.374e-04	7.202
3.317088	4.655e-04	7.302
3.317206	5.011e-04	6.963
3.317399	5.593e-04	7.138
3.317663	6.389e-04	6.968
3.317885	7.059e-04	6.913
3.317972	7.321e-04	6.858
3.318097	7.698e-04	6.693
3.318225	8.084e-04	6.562
3.318429	8.699e-04	6.581
3.318670	9.426e-04	6.702
3.318830	9.909e-04	6.573
3.318919	1.018e-03	6.624
3.319077	1.065e-03	6.661
3.319217	1.108e-03	6.493
3.319447	1.177e-03	6.449
3.319738	1.265e-03	6.279
3.320283	1.429e-03	6.528

TABLE VI: The dimensionless experimental measurements of the ^3He specific heat C_V^* . $T_c = 3.315545\text{K}$ was obtained from the joint fit of χ_T^* and C_V^* to the MSR ϕ^4 model.

T	$T/T_c - 1$	C_V^*
3.014570	-9.078e-02	7.881
3.021686	-8.863e-02	7.946
3.028699	-8.652e-02	7.959
3.035582	-8.444e-02	8.038
3.042383	-8.239e-02	8.088
3.049135	-8.035e-02	8.069
3.055774	-7.835e-02	8.173
3.059940	-7.709e-02	8.183
3.064174	-7.582e-02	8.200
3.070900	-7.379e-02	8.231
3.077578	-7.177e-02	8.312
3.081723	-7.052e-02	8.331
3.085888	-6.927e-02	8.332
3.092441	-6.729e-02	8.541
3.099071	-6.529e-02	8.471
3.103159	-6.406e-02	8.428
3.104792	-6.357e-02	8.498
3.106435	-6.307e-02	8.512
3.108071	-6.258e-02	8.498
3.109702	-6.208e-02	8.543
3.111329	-6.159e-02	8.578
3.112949	-6.110e-02	8.624
3.114572	-6.062e-02	8.528
3.115721	-6.027e-02	8.561
3.116924	-5.991e-02	8.622
3.120951	-5.869e-02	8.631
3.130580	-5.579e-02	8.680
3.143237	-5.197e-02	8.798
3.155746	-4.820e-02	8.902
3.165016	-4.540e-02	9.008
3.171098	-4.357e-02	9.061
3.177146	-4.174e-02	9.118
3.182946	-3.999e-02	9.177
3.188913	-3.819e-02	9.248
3.190517	-3.771e-02	9.231
3.191638	-3.737e-02	9.257
3.198331	-3.535e-02	9.419
3.210298	-3.174e-02	9.590
3.222044	-2.820e-02	9.760
3.235858	-2.403e-02	9.677
3.237019	-2.368e-02	9.888

3.320536	1.505e-03	6.285	3.400172	2.552e-02	4.736
3.320809	1.588e-03	6.270	3.402356	2.618e-02	4.727
3.320989	1.642e-03	6.261	3.404543	2.684e-02	4.720
3.321325	1.743e-03	6.209	3.406731	2.750e-02	4.718
3.321702	1.857e-03	6.096	3.408924	2.816e-02	4.710
3.322174	1.999e-03	5.919	3.411116	2.883e-02	4.701
3.322638	2.139e-03	6.104	3.412433	2.922e-02	4.666
3.323109	2.281e-03	5.910	3.413044	2.941e-02	4.661
3.323586	2.425e-03	5.944	3.413649	2.959e-02	4.737
3.324054	2.566e-03	5.853	3.414220	2.976e-02	4.723
3.324387	2.667e-03	5.711	3.414872	2.996e-02	4.681
3.324605	2.733e-03	5.867	3.415805	3.024e-02	4.678
3.324881	2.816e-03	5.874	3.417482	3.075e-02	4.674
3.325280	2.936e-03	5.802	3.419719	3.142e-02	4.661
3.325758	3.080e-03	5.776	3.421956	3.209e-02	4.660
3.326317	3.249e-03	5.741	3.424190	3.277e-02	4.651
3.327445	3.589e-03	5.682	3.426428	3.344e-02	4.645
3.328419	3.883e-03	5.649	3.428664	3.412e-02	4.631
3.329076	4.081e-03	5.485	3.430897	3.479e-02	4.630
3.329729	4.278e-03	5.666	3.433131	3.547e-02	4.632
3.331770	4.894e-03	5.507	3.435362	3.614e-02	4.647
3.332809	5.207e-03	5.440	3.437601	3.681e-02	4.628
3.333808	5.508e-03	5.465	3.439850	3.749e-02	4.626
3.334811	5.811e-03	5.397	3.442101	3.817e-02	4.620
3.335822	6.116e-03	5.382	3.444355	3.885e-02	4.609
3.336837	6.422e-03	5.337	3.446613	3.953e-02	4.597
3.337850	6.727e-03	5.329	3.448872	4.021e-02	4.592
3.338592	6.951e-03	5.308	3.451131	4.089e-02	4.594
3.339364	7.184e-03	5.301	3.453395	4.158e-02	4.584
3.340384	7.492e-03	5.277	3.455659	4.226e-02	4.576
3.341933	7.959e-03	5.241	3.459058	4.328e-02	4.579
3.344007	8.585e-03	5.199	3.463590	4.465e-02	4.570
3.346105	9.217e-03	5.161	3.468123	4.602e-02	4.557
3.348203	9.850e-03	5.142	3.472658	4.739e-02	4.562
3.350301	1.048e-02	5.112			
3.352403	1.112e-02	5.085			
3.354507	1.175e-02	5.051			
3.356612	1.239e-02	5.022			
3.357923	1.278e-02	5.015			
3.358726	1.302e-02	4.987			
3.359605	1.329e-02	5.006			
3.361045	1.372e-02	4.992			
3.363198	1.437e-02	4.967			
3.365356	1.502e-02	4.949			
3.367521	1.568e-02	4.931			
3.369688	1.633e-02	4.909			
3.371862	1.699e-02	4.884			
3.374039	1.764e-02	4.875			
3.375402	1.805e-02	4.917			
3.376038	1.825e-02	4.857			
3.376954	1.852e-02	4.862			
3.378597	1.902e-02	4.845			
3.380724	1.966e-02	4.836			
3.382861	2.030e-02	4.820			
3.385006	2.095e-02	4.812			
3.387156	2.160e-02	4.803			
3.389310	2.225e-02	4.789			
3.391472	2.290e-02	4.774			
3.393640	2.355e-02	4.766			
3.395811	2.421e-02	4.765			
3.397990	2.487e-02	4.738			

TABLE VII: The experimental measurements of the ^3He reduced density $\Delta\rho_{L,V}$ along the coexistence curve. The data was provided by Prof. H. Meyer as it was used in ref. [12]. The index = 0, 8 corresponds to liquid and vapor respectively.

$T/T_c - 1$	$ \Delta\rho_{L,V} $	index
2.848e-04	7.192e-02	0
3.128e-04	7.460e-02	0
3.445e-04	7.705e-02	0
3.836e-04	7.972e-02	0
4.460e-04	8.365e-02	0
5.319e-04	8.859e-02	0
5.322e-04	8.826e-02	0
5.963e-04	9.177e-02	0
6.638e-04	9.512e-02	0
7.279e-04	9.822e-02	0
8.332e-04	1.028e-01	0
9.630e-04	1.089e-01	0
9.658e-04	1.084e-01	0
1.279e-03	1.198e-01	0
1.399e-03	1.235e-01	0
1.430e-03	1.239e-01	0
1.518e-03	1.270e-01	0
2.171e-03	1.438e-01	0
2.421e-03	1.494e-01	0

3.255e-03	1.657e-01	0	1.500e-02	2.857e-01	8
3.862e-03	1.761e-01	0	1.934e-02	3.140e-01	8
4.066e-03	1.793e-01	0	2.485e-02	3.438e-01	8
4.868e-03	1.908e-01	0	2.880e-02	3.617e-01	8
6.266e-03	2.090e-01	0	3.157e-02	3.747e-01	8
7.261e-03	2.207e-01	0	3.505e-02	3.897e-01	8
9.366e-03	2.420e-01	0	3.827e-02	4.021e-01	8
1.319e-02	2.738e-01	0	4.388e-02	4.226e-01	8
1.834e-02	3.081e-01	0	5.599e-02	4.619e-01	8
2.285e-02	3.340e-01	0	7.054e-02	5.023e-01	8
2.854e-02	3.626e-01	0	7.474e-02	5.123e-01	8
3.135e-02	3.755e-01	0	8.388e-02	5.347e-01	8
3.496e-02	3.911e-01	0	9.639e-02	5.623e-01	8
3.783e-02	4.027e-01	0	1.467e-01	6.502e-01	8
4.348e-02	4.232e-01	0	2.096e-01	7.309e-01	8
5.230e-02	4.463e-01	0	2.627e-01	7.854e-01	8
5.320e-02	4.474e-01	0	3.267e-01	8.368e-01	8
5.559e-02	4.636e-01	0	3.927e-01	8.802e-01	8
6.988e-02	5.038e-01	0	5.547e-01	9.589e-01	8
7.140e-02	5.124e-01	0	6.773e-01	9.766e-01	8
7.389e-02	5.135e-01	0	8.272e-01	9.618e-01	8
8.380e-02	5.381e-01	0	9.960e-01	9.989e-01	8
9.589e-02	5.656e-01	0			
1.025e-01	5.749e-01	0			
1.034e-01	5.800e-01	0			
1.339e-01	6.363e-01	0			
1.710e-01	6.887e-01	0			
2.227e-01	7.524e-01	0			
3.106e-01	8.389e-01	0			
4.970e-01	9.499e-01	0			
5.850e-01	9.813e-01	0			
6.980e-01	1.007e+00	0			
7.580e-01	1.016e+00	0			
8.190e-01	1.018e+00	0			
8.790e-01	1.019e+00	0			
9.390e-01	1.019e+00	0			
9.980e-01	1.017e+00	0			
8.433e-04	1.039e-01	0			
8.995e-04	1.062e-01	0			
9.060e-04	1.058e-01	0			
1.221e-03	1.172e-01	0			
1.515e-03	1.264e-01	8			
1.611e-03	1.300e-01	8			
1.647e-03	1.302e-01	8			
1.729e-03	1.330e-01	8			
1.791e-03	1.342e-01	8			
1.931e-03	1.375e-01	8			
2.075e-03	1.417e-01	8			
2.315e-03	1.473e-01	8			
2.382e-03	1.478e-01	8			
2.661e-03	1.545e-01	8			
2.849e-03	1.585e-01	8			
3.085e-03	1.625e-01	8			
3.693e-03	1.731e-01	8			
4.713e-03	1.890e-01	8			
5.169e-03	1.950e-01	8			
6.004e-03	2.057e-01	8			
6.811e-03	2.153e-01	8			
7.311e-03	2.205e-01	8			
8.153e-03	2.294e-01	8			
1.314e-02	2.727e-01	8			

-
- [1] R. Schloms and V. Dohm, Nuclear Physics **B328**, 639 (1989).
- [2] C. Bagnuls and C. Bervillier, Phys. Rev. B **32**(11), 7209 (1985).
- [3] R. Guida and J. Zinn-Justin, J. Phys. A **31**, 8103 (1998).
- [4] S. A. Larin, M. Mönnigmann, M. Strösser, and V. Dohm, Phys. Rev. B **58**(6), 3394 (1998).
- [5] C. Bagnuls and C. Bervillier, lanl.arXiv.org **hep-th**, 0112209 (2002).
- [6] R. Schloms and V. Dohm, Phys. Rev. B **42**, 6142 (1990).
- [7] F. J. Halfkann and V. Dohm, Z. Phys. B - Condensed Matter **89**, 79 (1992).
- [8] H. J. Krause, R. Schloms, and V. Dohm, Z. Phys. B - Condensed Matter **79**, 287 (1990).
- [9] M. Fisher and S.-Y. Zinn, J. Phys. A **31**(37), L629 (1998).
- [10] I. Hahn, F. Zhong, M. Barmatz, R. Haussmann, and J. Rudnick, Phys. Rev. E **63**, 055104 (2001).
- [11] M. Barmatz, I. Hahn, F. Zhong, M. Anisimov, and V. Agayan, J. Low Temp. Phys. **121**, no.5-6, 633 (2000).
- [12] E. Luijten and H. Meyer, Phys. Rev. E **62**, 3257 (2000).
- [13] Y. Miura, H. Meyer, and A. Ikushima, J. Low Temp. Phys. **55**, 247 (1984).
- [14] R. P. Behringer, A. Onuki, and H. Meyer, J. Low Temp. Phys. **81**, 71 (1990).
- [15] R. G. Brown and H. Meyer, Phys. Rev. A **6**, 364 (1972).
- [16] C. Pittman, T. Doiron, and H. Meyer, Phys. Rev. B **20**, 3678 (1979).
- [17] A. Povodyrev, M. A. Anisimov, and J. V. Sengers, Physica A **264**(3-4), 345 (1999).
- [18] H. Meyer, 2000 NASA/JPL Conference on Fundamental Physics in Microgravity **NASA Document D-21522**, 33 (2001).
- [19] D. B. Roe and H. Meyer, J. Low Temp. Phys. **30**, 91 (1978).
- [20] V. Agayan, M. Anisimov, and J. Sengers, Phys. Rev. E **64**(2), 026125/1 (Aug. 2001).
- [21] M. Barmatz, *MISTE science requirements document*, JPL-D17083 (2000).
- [22] I. Hahn, *COEX science requirements document*, JPL-D23024 (2002).